Title
ANOMALOUS L-SUBSHELL RATIOS IN MIXED M1-E2 TRANSISTIONS

Authors
Novakov, T.
Hollander, J.M.

Publication Date
1964-05-01

UCRL-11400

University of California

Ernest O. Lawrence Radiation Laboratory

ANOMALOUS L-SUBSHELL RATIOS IN MIXED M1-E2 TRANSITIONS

Berkeley, California

DISCLAIMER

Rept. sub. for pub. in Nuclear Physics.

UCRL-11400

UNIVERSITY OF CALIFORNIA

Lawrence Radiation Laboratory
Berkeley, California

AEC Contract No. W-7405-eng-48

ANOMALOUS L-SUBSHELL RATIOS IN MIXED M1-E2 TRANSITIONS

T. Novakov and J. M. Hollander

May 1, 1964

ANOMALOUS L-SUBSHELL RATIOS IN MIXED M1-E2 TRANSITIONS*

T. Novakov† and J. M. Hollander

Lawrence Radiation Laboratory
University of California
Berkeley, California

May 1, 1964

Abstract

L-subshell ratios of a number of M1-E2 transitions have been measured accurately with the Berkeley 50-cm. iron-free $\pi\sqrt{2}$ spectrometer. When the three L-subshell conversion lines are resolved, the M1-E2 mixing ratio is overdetermined, because a unique value of δ^2 (i.e. E2/M1) is given by any one of the ratios: L_I/L_{II}, L_I/L_{III} and L_{II}/L_{III}. (Algebraically only two of these ratios are independent.) Thus, if all three ratios are measured experimentally, the same value of δ^2 should in principle be obtained. In fact, this does not always appear to be the case. One of the most pronounced discrepancies is found in the case of the 103 keV transition in Eu^{153}. The measured ratios are $L_I/L_{II} = 8.22 \pm 0.10$, $L_I/L_{III} = 20.65 \pm 0.28$, and $L_{II}/L_{III} = 2.51 \pm 0.05$. With use of carefully interpolated values from Sliv's tables, the E2 admixtures obtained are: 2.02 ± 0.08, 1.66 ± 0.03 and 1.44 ± 0.06 percent, respectively. With Rose's values the E2 admixtures are 2.18 ± 0.08, 1.52 ± 0.03 and 1.15 ± 0.06 percent. Similar discrepancies were observed in the 114 keV transition in Lu^{175} and 42 and 52 keV transitions in Bk^{249}. Relatively good agreement with Sliv's values is found for the 69 keV transition in Eu^{153} and for the 58 keV transition in Tb^{159}. The agreement is generally better with Sliv's than with Rose's values. The two sets of theoretical L conversion coefficients differ sometimes by as much as 50 percent.

ANOMALOUS L-SUBSHELL RATIOS IN MIXED M1-E2 TRANSITIONS

T. Novakov and J. M. Hollander

Lawrence Radiation Laboratory
University of California
Berkeley, California

May 1, 1964

1. Introduction

During recent years the process of internal conversion of gamma rays has been and still is the subject of many theoretical and experimental investigations. Measurements of internal conversion coefficients (ICC) for a particular electron shell, or ICC ratios for different electron shells (for example $K:\Sigma L$, $L_I:L_{II}:L_{III},\ldots$) and comparison of the results with the tabulated theoretical values have yielded significant information about the multipole orders of nuclear transitions. At the time of the earliest theoretical works on internal conversion it was believed that ICC are independent of the details of nuclear structure. Therefore it was considered that ICC calculations may be carried out without any assumptions about nuclear structure, by using only requirements imposed by energy, angular momentum and parity conservation. This procedure is expected to remain valid as long as the electron penetration into nuclear matter is not appreciable.

The first tabulated theoretical ICC for K, L_I, L_{II} and L_{III} shells were those of Rose, et al.[1]). Rose used electron wave functions appropriate for a point nuclear charge distribution. The confinement of the nuclear currents to the origin resulted in the vanishing of all penetration terms.

Because of improvements in the techniques of measurement significant deviations of experimentally determined ICC from the theoretical values were

subsequently found, particularly for M1 transitions. These discrepancies have been explained by Sliv[2,3]) who attributed them to the effect of finite nuclear size. Sliv and Band[4]) evaluated the finite penetration terms by assuming a very simple nuclear model in which the nuclear transition currents lie on the spherical nuclear surface, and use was made of electron wave functions appropriate for a finite static nuclear charge distribution in calculation of the finite--size--corrected ICC. In this "surface-current" model the penetration term is constant and therefore computation of the ICC is practical. The resulting ICC are, as before, independent of nuclear matrix elements. An alternative method to include the effect of finite nuclear size was used by Rose[5]) who set the penetration terms equal to zero while evaluating the principal conversion matrix element. The electron wave functions were again those appropriate for a finite charge distribution. This has been called the "no-penetration" model.

These finite-size corrected tables are remarkably accurate, so much in fact that a considerable effort has been expended, a good part in vain, to find disagreements between theory and experiment. However in some cases and for certain multipolarities definite disagreements have been found, far outside the experiment errors. From the theoretical work of Church and Weneser[6]) it becomes clear that the independence of the ICC from the details of nuclear structure is valid only when the gamma ray emission is not highly hindered with respect to the "single-particle" transition rate. If the gamma ray emission is hindered, while the electron part is not correspondingly hindered, then ICC may in an essential way depend on the nuclear matrix elements. Under these circumstances the usually small contributions of the penetrating electrons to the internal conversion process may become significant. Therefore high precision ICC studies, in cases where the multipolarity is already known, can in principle be used for exploring the finer details of nuclear structure.

A large amount of experimental and theoretical work has been devoted to the study of the influence of nuclear structure on the process of internal conversion. In general two distinct classes of transitions have been examined:

(1) Highly retarded transitions. In these cases the full influence of the penetration effects may be expected. In the case of very slow electric dipole transitions large anomalies have been observed in the L_I and L_{II} shell conversion[7]). The most spectacular example is the 85 keV transition in Pa^{231} for which the observed L_I and L_{II} ICC are 10 to 20 times higher than the tabulated values, while the L_{III} conversion is normal. A correlation was established between the deviations of the ICC and the inhibition of the gamma ray matrix element. More recently a similar study has been made of some E1 transitions in the rare earth region[8]).

There is also considerable evidence, from ICC measurements and electron-gamma angular correlation studies, of the effect of nuclear structure on internal conversion of moderately retarded $\Delta\ell$-forbidden M1 transitions[9]).

Some evidence concerning the observation of a nuclear structure effect on L subshell conversion ratios has also been reported[10]).

(2) Fast transitions. Much effort has gone into the measurement of the K shell ICC of E2 transitions, which are generally fast[11]). The fact that there appears to be good agreement in most cases between theory and experiment for the K conversion has been taken as evidence of the essential correctness of the Sliv and Rose theoretical calculations. However, the situation is not so clear for the L subshell conversion, where some disagreements have been reported[12]).

It is interesting to examine the situation between these two extremes, to look for anomalies in ICC of transitions neither very slow nor very fast.

In this paper we report the results of a study of the L-subshell conversion coefficient ratios of some mixed M1-E2 transitions, carried out with the Berkeley high-resolution 50-cm iron-free $\pi\sqrt{2}$ spectrometer. The measurement of absolute values of ICC to better than 5% is not an easy job, but with the present techniques, determination of conversion ratios, expecially L-subshell conversion ratios, can easily be done with an accuracy of 1-2%. Knowledge of only the conversion ratios can of course not establish any absolute ICC values, but is was to be hoped that a systematic study of L-conversion ratios would reveal trends in observed deviations from theory, if any, from which the sources of the deviations might be understood.

An additional motivation for the careful study of mixed M1-E2 transitions derives from the practical necessity to have accurate values of the intensity of the smaller component (usually a few percent E2) for use in transition probability correlations with nuclear models, as for example the E2 branching ratio between cascade and crossover transitions within a rotational band, Also, the interpretation of gamma-gamma angular correlation data with mixed M1-E2 transitions may depend quite sensitively on the percentage of E2 admixture, so it is important to know this quantity with high accuracy.

2. Sources and Apparatus

Sources of Eu^{153}, Gd^{159}, Yb^{175}, Lu^{177}, W^{187}, and Es^{253} were used in this work. All isotopes other than Es^{253} were produced by reactor irradiation of the corresponding electromagnetically enriched stable isotope* (as oxide)

*The enriched isotopes were obtained from the Stable Isotopes Division, Oak Ridge National Laboratory, Oak Ridge, Tennessee.

in either the Materials Testing Reactor, Arco Idaho, or the G. E. Reactor, Valecitos, California. The Es^{253} activity was separated from the products of a long-term neutron irradiation of heavy isotopes (principally Cm^{244}) in the Materials Testing Reactor. Sources for the spectrometer were prepared by vacuum sublimation of dried chlcride solution from a shaped tungsten boat at $\geq 2000^{\circ}$ C, through a collimator (1mm × 10 mm and/or 0.5 mm × 10 mm) on to aluminum foil backing of surface density ~ 3.5 mg/cm^2.

The conversion electrons were magnetically analyzed with the Berkeley 50-cm radius $\pi\sqrt{2}$ iron-free double focusing spectrometer[13,14]. The detector was a side window Geiger counter having a measured dead time of ≈ 50 μsec. The counter aperture, 1 mm × 20 mm, was covered with a two-layer Formvar film of surface density ≈ 50 μgm/cm^2, which was 100% transparent for the electron energies of interest. The spectrometer current is programmed automatically and the output data recorded by an electric typewriter. The reliability of the counting system was increased by employing three parallel scalers to record the output data.

It is essential for this type of measurement that the current stability of the spectrometer be extremely good. This was checked daily during all experiments. The short-term current drift (over periods of hours) has usually been less than a few parts in 10^5; on those occasions when greater instabilities were noted, counting was terminated until the fault was corrected. Figure 1 shows a plot of the spectrometer current, measured over a period of two hours with a Guildline No. 9144 precision potentiometer.

Two fixed spectrometer baffles were used, corresponding to aperture solid angles of $\Omega/4\pi = 0.08\%$ and $\Omega/4\pi = 0.16\%$ and focusing aberrations of 0.05% and 0.1%, respectively. The achieved line-widths varied from 0.05%

(in momentum) to 0.15% because of differences of source quality and electron energy. (The line width from Es^{253} was additionally broadened, to 0.28%, partly because of alpha recoil effects.) In all cases, the resolution was sufficient to resolve L_I and L_{II} conversion lines from each other.

3. Relative Conversion Electron Line Intensity Determinations

The experimental procedure followed in this study was the precise determination of the relative intensities of L_I, L_{II} and L_{III} conversion lines from a number of mixed M1-E2 transitions in the energy region 40 to 150 keV. In each experiment, the energy region of the L conversion lines was scanned at least three times, with equal current increments. After subtraction of the constant counter background (18/min), decay corrections were applied to each measured point. The source intensity and spectrometer baffle were so chosen that the peak counting rates were sufficiently low that dead time corrections were unnecessary. A typical run representing the L subshell conversion lines of the 103 keV transition in Eu^{153} is shown in fig 2. The same spectrum plotted on semi logarithmic scale (after subtraction of the beta continuum background) is reproduced in fig. 3.

Integration of the conversion line areas was always carried out between current limits on both sides of the peak position, at which the counting rates were equal to one percent of the peak counting rate (see fig. 3). In cases where there was no interference from neighboring lines the integration consisted simply of the summation of all counting rates between the above mentioned limits. This is justified because all successive points are separated by the same current increment. The constancy of these increments is assured by the high operating stability of the current generation and control system.

In cases where the relative separation between conversion lines is small the contribution from neighboring lines has to be taken into account. This is done by the use of semi-log plots similar to that of fig. 3. The line shape on such a plot is found to be independent of the line intensity. That line which is least disturbed from other lines can then be used to determine the "standard" line shape. In the case of fig. 3 the L_I line shape was used as the standard. As can be seen from the figure the influence of the L_{II} and L_{III} line shapes on the L_I line shape is at most 1-2%. Therefore the L_I line shape (solid line in fig. 3) can be used with some confidence to estimate the low energy tails of the other two lines.

The total intensity of the L_{III} line in fig. 3 is therefore obtained from the direct addition of experimental points over the region where no extrapolation was used (solid line) and from the addition of equidistant points read from the extrapolated line representing the low energy tail (dashed line).

The L_{II} line intensity determination was made by subtracting that part of the extrapolated L_{III} line tail which falls in the L_{II} integration region as defined earlier. In the case of the L_I line contributions from both L_{II} and L_{III} lines were subtracted.

The areas determined by the above procedure were divided by the corresponding peak-position currents.

The experimental error attached to our quoted intensity values includes the statistical error as well as the errors from low-energy tail extrapolation and background subtraction. We have attached an arbitrary 10 % error to all numbers obtained from extrapolations using the "standard" line shape. The total error ΔN is then composed as follows

$$\Delta N = \pm\sqrt{N_d + n \cdot N_b + (N_{ext} \cdot 0.1)^2 + (N_t \cdot 0.1)^2} \quad .$$

Here N_d is the direct sum of the experimental points where no extrapolation was used. N_b is the background subtracted from each point and n is the total number of points describing the line. N_{ext} is the part of the intensity obtained by addition of points on the extrapolated line tail. N_t is the extrapolated contribution from the tails of other, higher energy, lines. The errors of the conversion ratios are obtained in the usual way from the line intensities and their errors.

4. Discussion of Results

When the three L-subshell conversion lines are resolved, the M1-E2 mixing ratio is overdetermined because a unique value of $\delta^2 (\equiv E2/M1)$ is given by any one of the ratios: L_I/L_{II}, L_I/L_{III}, and L_{II}/L_{III}. (Only two of these ratios are algebraically independent, of course). Thus, if all three ratios are measured experimentally, the same value of δ^2 should in principle be obtained.

In fact, this does not always appear to be the case. Figures 4-11 illustrate the actual situation. In these figures the variations of the theoretical L_I/L_{II}, L_I/L_{III}, and L_{II}/L_{III} ratios as a function of the percentage E2 admixture are represented. In figures 4-9 the theoretical L-subshell ICC of both Rose and of Sliv and Band were used. Data for Bk^{249} (figs. 10 and 11) were analyzed only with Sliv's values because Rose's tabulation does not extend to Z = 97. Horizontal bands represent the

experimental L-subshell conversion ratios while the vertical shaded bands give the amount of the E2 admixture in percent, as obtained from each subshell conversion ratio.

From figs. 4-11 it can be seen that the E2 admixtures determined from different L-subshell conversion ratios show deviations which in many cases are beyond the limits of experimental error. No obvious systematic trend in these deviations has been noted. As an example, in the case of the two transitions in Eu^{153}, the lowest percent E2 is obtained from the L_I/L_{II} ratio of the 69 keV transition whereas the highest percent E2 is obtained from the L_I/L_{II} ratio of the 103 keV transition. The two cascade transitions in Bk^{249} that belong to the same rotational band also show this kind of discrepancy. The different degrees of discrepancy obtained by use of Rose's tables and those of Sliv and Band are obvious; except in one case (Lu^{175}) all transitions show discrepancies when Rose's tables are used.

A number of factors can possibly contribute to the observed discrepancies in E2 admixtures. The accuracy of the experimental data has already been discussed and the error limits are shown in Table 1 and in the figures. Some degree of computational inaccuracy is expected in the theoretical conversion coefficients and it is essential to consider this before any conclusions are drawn from the experimental data. Sliv[15]) has pointed out that the computational accuracy of the L-subshell conversion coefficients in the Sliv and Band tables is thought to be $\pm 2\%$. Some additional uncertainty, possibly 2-3%, may be introduced by the interpolation between the tabulated values. Thus it may be reasonable to expect uncertainties of 5-6% in interpolated theoretical values of the L-subshell ratios. If, after consideration of these uncertainties, inconsistent results are still obtained, then either the errors in tabulated values are greater than quoted (because of errors in computation or in the

physical assumptions) or some effects not taken into account in the calculations are appearing, for example, structural effects of the finite nuclear size.

In two of the measured transitions, the 103-keV in Eu^{153} and the 52-keV in Bk^{249}, the energies are almost exactly equal to the tabulated energies (k = 0.2 and 0.1, respectively) so the error introduced by interpolation can in these cases be neglected, and the analysis of the data is more meaningful. In fig. 12 the experimental ratios for the 103 keV transition in Eu^{153} are compared with the theoretical values of Sliv and Band and of Rose, with the assumption of a ± 2% error in the theoretical subshell coefficients. The bands representing the resulting E2 admixtures are naturally now wider than before. In the comparison with Sliv and Band, there is still no overlap of the admixture band obtained from the L_I/L_{II} ratio with the other two bands. The L_{II}/L_{III} and L_I/L_{III} bands overlap marginally. In the comparison with Rose, a more obvious disagreement exists.

In fig. 13 a similar analysis is made of the 52 keV transition in Bk^{249}. The E2 admixture bands from the L_I/L_{II} and L_{II}/L_{III} ratios do not overlap but there is marginal overlap of the L_I/L_{III} band with the other two. No comparison with Rose is made because of the lack of theoretical values for Z = 97.

A few words should be said about the interpolation procedure used in analyzing the other cases. The interpolated values for M1 conversion coefficients were obtained by plotting log $K^3 \beta_1$ vs log k; the resulting smooth and regular curves allowed accurate interpolation. For E2 conversion, log $K^2\alpha_2$, log $K^3\alpha_2$, and log $K^5\alpha_2$ were plotted against log k. For each case the exponent giving the smoothest and most regular curve was used. We believe that the error due to interpolation by the above procedure is not greater than 1%.

Let us consider further the experimental results with reference to the Sliv and Band theoretical coefficients. Although all the observed

deviations can be called "small", the general agreement appears better for the 69 keV transition in Eu^{153}, 58 keV transition in Tb^{159}, or 134 keV transition in Re^{187}, than it is for the 103 keV transition in Eu^{153}, 114 keV transition in Lu^{175}, or both the 42 and 52 keV transitions in Bk^{249}. The agreement is also relatively poor for the 113 keV transition in Hf^{177}, although in this case the L-subshell ratios are rather insensitive to the mixing ratio because of the high E2 admixture. In Eu^{153}, the 69 keV transition, for which there is "agreement", is a rotational transition with an M1-photon hindrance factor[16] of only 12, whereas the 103 keV transition, for which there is "disagreement", is a slower interband transition, with an M1-photon hindrance factor of 420[16]. If a correlation of this type were in fact noted from further experimental data, it would constitute evidence for a nuclear structure effect on the internal conversion of these predominantly M1 transitions, for nuclear structure effects, if present, should affect differently the different electron shells[17]. The measurement of L-subshell conversion coefficients or intensity ratios might be a sensitive tool with which to study such effects in moderately fast transitions.

The 58 keV transition in Tb^{159} and the 134 keV transition in Re^{187} show "agreement", and both are relatively fast transitions, with M1-photon hindrance factors 23 and ~ 1, respectively[18,19].

A transition in which the M1-component is quite hindered is the 113 keV in Hf^{177} (M1-photon hindrance factor of ~ 2000[20]). As mentioned earlier, this transition is almost pure E2 so the L-subshell ratios are rather insensitive to small changes in the M1-component. Nonetheless, the experimental data are precise enough to show a "disagreement": The experimental L_{II}/L_{III} ratio is lower even than the theoretical ratio for a pure E2 transition, hence it is inconsistent with any amount of M1 (which would raise the L_{II}/L_{III} ratio).

The other two conversion ratios give a consistent E2 admixture (between 91.1% and 92.7%). The mixing ratio has been determined independently by angular correlations by Thun et al.[21] who find $10 \leq |\delta| \leq 4$, which corresponds to an E2 admixture between 93.5% and 99%. Other reported values deviate still more from our result[22]). It is interesting to note that this transition is one of the rare examples of a rotational transition in which a near equality of the gyromagnetic ratios for rotation and particle structure causes a large reduction in the M1-transition probability and makes likely a nuclear structure effect on the internal conversion[23]).

The 114 keV transition in Lu^{175} is another case of "disagreement", although the M1-photon hindrance factor is only about 20[20]). The two transitions in Bk^{249} show "disagreement", but the hindrance factors here are not well established.

The preceding comparisons have been with the tables of Sliv and Band. If the above data are compared with the theoretical coefficients of Rose, it is found that all cases except the 114 keV transition in Lu^{175} show "disagreement". The 103 keV transition in Eu^{153} shows a serious disagreement.

The present situation appears highly unsatisfactory from a theoretical point of view because of gross deviations between the Rose theoretical coefficients and those of Sliv and Band, which naturally complicate the interpretation of experimental results. These deviations can be as much as 50% between the values from the two theoretical tables. This situation is illustrated in figs. 14 and 15 where the ratios of Sliv's and Rose's L-ICC are plotted against atomic number and energy.

To make possible further interpretation of the data presented here information about the absolute experimental L-subshell ICC are needed. Also M1/E2 mixing ratios determined independently of internal conversion would be valuable. Reduction in the calculational uncertainties in the theoretical

L-subshell conversion coefficients, as well as much more closely spaced theoretical values, would also be desirable.

We wish to thank Dr. R. L. Graham for his help during the early part of this investigation and to acknowledge several valuable discussions with Professor J. O. Rasmussen. The technical assistance of C. J. Butler, J. A. Harris, D. S. McClure, and P. Salz is also gratefully acknowledged. One of us (T. N.) wishes to record his gratitude to Professor I. Perlman for his kind hospitality and that of all members of the Nuclear Chemistry Division during his stay at the Laboratory.

References and Footnotes

*Work done under the auspices of the U. S. Atomic Energy Commission.

†On leave from the Faculty of Sciences, University of Belgrade, Yugoslavia.

1. M. E. Rose, G. H. Goertzel, B. I. Spinrad, J. Harr, and P. Strong, Phys. Rev. 76, (1949) 1883
2. L. A. Sliv, JETP (USSR) 21 (1951) 770
3. L. A. Sliv and M. A. Listengarten, JETP (USSR) 22 (1952) 29
4. L. A. Sliv and I. M. Band, Coefficients of Internal Conversion of Gamma-Radiation (USSR Academy of Sciences, Moscow-Leningrad, 1956) Part I: K Shell, Part II: L-Shell. See also Gamma Rays, edited by L. A. Sliv, (USSR Academy of Sciences, Moscow-Leningrad, 1961)
5. M. E. Rose, Internal Conversion Coefficients, (North-Holland Publishing Co., Amsterdam, 1958)
6. E. L. Church and J. Weneser, Phys. Rev. 104, (1956) 1382
7. F. Asaro, F. S. Stephens, J. M. Hollander, and I. Perlman, Phys. Rev. 117 (1960) 492
8. C. J. Herrlander and G. T. Ewan, Talk given at the Converence on the Role of Atomic Electrons in Nuclear Transformations, Warsaw, 1963
9. See, for example, T. R. Gerholm, B.-G. Petterson, B. Van Nooijen, and Z. Grabowski, Nucl. Phys. 24 (1961) 177
10. T. Novakov and R. Stepić, Physics Letters 3 (1962) 82
11. S. Hultberg, Nucl. Phys. (to be published)
12. C J. Herrlander and R. L. Graham, Nucl. Phys. (to be published)
13. K. Siegbahn, C. L. Nordling, and J. M. Hollander, UCRL-10023 (January 1962)
14. J. M. Hollander and R. L. Graham, UCRL-10624 (January 1963)
15. L. A. Sliv, private communication to J. M. Hollander, (December 1963)

16. T. Suter, P. Reyes-Suter, S. Gustafsson, and I. Marklund, Nucl. Phys. 29 (1962) 33

17. E. L. Church and J. Weneser, Bull. Am. Phys. Soc. 7 (1962) 490

18. E. E. Berlovich, M. P. Bonitz and V. V. Nikitin, Izv. Akad. Nauk SSSR, Ser. Fiz. 25 (1961) 218

19. C. J. Gallagher, Jr., W. F. Edwards and G. Manning, Nucl. Phys. 19 (1960) 181

20. J. Lindskog, T. Sundström and P. Sparrman, Arkiv Fysik 23 (1963) 341

21. J. E. Thun, Z. Grabowski, W. D. Hamilton, and M. S. El-Nesr, Nucl. Phys. 29 (1962) 13

22. H. I. West, Jr., L. G. Mann, R. J. Nagle, Phys. Rev. 124 (1961) 527

23. A. S. Reiner, Nucl. Phys. 5, (1958) 544

Table I.

E2 admixtures inferred from experimental L-subshell conversion ratios and the theoretical L-subshell ICC of Rose and of Sliv.

Nucleus	Transition Energy	Exp. L subshell ratios $L_I:L_{II}$	Exp. L subshell ratios $L_I:L_{III}$	Exp. L subshell ratios $L_{II}:L_{III}$	E2 admixture (%) from L subshell ratios: Rose[a] $L_I:L_{II}$	Rose[a] $L_I:L_{III}$	Rose[a] $L_{II}:L_{III}$	Sliv[b] $L_I:L_{II}$	Sliv[b] $L_I:L_{III}$	Sliv[b] $L_{II}:L_{III}$
Eu^{153}	69 keV	6.35 ± 0.13	9.85 ± 0.09	1.55 ± 0.03	1.88 ± 0.07	1.73 ± 0.03	1.56 ± 0.10	1.81 ± 0.10	1.87 ± 0.03	2.00 ± 0.12
		6.22 ± 0.08	9.87 ± 0.10	1.59 ± 0.03[c]						
Eu^{153}	103 keV	8.22 ± 0.10	20.65 ± 0.28	2.51 ± 0.05	2.18 ± 0.07	1.52 ± 0.03	1.15 ± 0.06	2.02 ± 0.08	1.66 ± 0.03	1.44 ± 0.06
		8.42 ± 0.09	20.86 ± 0.37	2.47 ± 0.05[c]						
Tb^{159}	58 keV	5.96 ± 0.21	9.47 ± 0.29	1.59 ± 0.07	1.52 ± 0.08	1.29 ± 0.04	1.02 ± 0.12	1.43 ± 0.12	1.40 ± 0.05	1.37 ± 0.13
Lu^{175}	114 keV	2.46 ± 0.03	3.24 ± 0.03	1.32 ± 0.02	16.70 ± 0.15	16.55 ± 0.10	15.65 ± 0.35	17.15 ± 0.15	18.25 ± 0.05	21.6 ± 0.50
Hf^{177}	113 keV	0.186 ± 0.004	0.204 ± 0.004	1.098 ± 0.003	91.7 ± 0.5	91.8 ± 0.5	---	91.6 ± 0.5	92.2 ± 0.5	---
Re^{187}	134 keV	7.86 ± 0.12	26.86 ± 0.32	3.42 ± 0.07	2.97 ± 0.12	2.50 ± 0.07	2.25 ± 0.11	2.52 ± 0.14	2.67 ± 0.05	2.76 ± 0.11
Bk^{249}	42 keV	3.47 ± 0.03	8.36 ± 0.13	2.41 ± 0.04	---	---	---	1.97 ± 0.06	1.76 ± 0.03	1.48 ± 0.07
Bk^{249}	52 keV	4.35 ± 0.03	11.33 ± 0.16	2.60 ± 0.04	---	---	---	1.79 ± 0.05	1.98 ± 0.03	2.23 ± 0.09

[a] Reference 5.

[b] Reference 4.

[c] R. L. Graham, Private communication (September 1963).

UCRL-11400

Figure Captions

Figure 1. Test of Current Stability of Iron-Free Spectrometer Power Supply, over a period of about 2 hours. The magnet current was measured with a Guildline Potentiometer, type No. 9144, with use of 0.01 ohm Leeds and Northrup series resistor kept at a temperature of $32.2^{\circ} \pm 0.05^{\circ}$ C.

Figure 2. L conversion lines of the 103 keV transition in Eu^{153} measured with 0.08% resolution in 50-cm iron-free $\pi\sqrt{2}$ spectrometer.

Figure 3. Data from fig. 2 plotted on a semi-log scale. The solid line describing the L_I line was used as the "standard" line shape to determine the low energy tails of the other two lines. The integration limits for the L_{III} line are indicated. The dashed line was obtained by using the "standard" line shape.

Figure 4. E2 admixtures (in percent) obtained from the three experimental L-subshell conversion ratios and the theoretical L subshell ICC of Sliv and of Rose for the 69 keV transition in Eu^{153}.

Figure 5. E2 admixtures (in percent) obtained from the three experimental L-subshell conversion ratios and the theoretical L subshell ICC of Sliv and of Rose for the 103 keV transition in Eu^{153}.

Figure 6. E2 admixtures (in percent) obtained from the three experimental L-subshell conversion ratios and the theoretical L-subshell ICC of Sliv and of Rose for the 58 keV transition in Tb^{159}.

Figure 7. E2 admixtures (in percent) obtained from the three experimental L-subshell conversion ratios and the theoretical L-subshell ICC of Sliv and of Rose for the 114 keV transition in Lu^{175}.

Figure 8. E2 admixtures (in percent) obtained from the three experimental L-subshell conversion ratios and the theoretical L-subshell ICC of Sliv and of Rose for the 113 keV transition in Hf^{177}. E2 admixture obtained by angular correlations (ref. 21) is indicated.

Figure 9. E2 admixtures (in percent) obtained from the three experimental L-subshell conversion ratios and the theoretical L-subshell ICC of Sliv and of Rose for the 134 keV transition in Re^{187}.

Figure 10. E2 admixtures (in percent) obtained from the three experimental L-subshell conversion ratios and the theoretical L-subshell ICC of Sliv for the 42 keV transition in Bk^{249}.

Figure 11. E2 admixtures (in percent) obtained from the three experimental L-subshell conversion ratios and the theoretical L-subshell ICC of Sliv for the 52 keV transition in Bk^{249}.

Figure 12. The data of fig. 5 with the inclusion of a $\pm$ 2% error in the partial theoretical L-subshell ICC.

Figure 13. The data of fig. 11 with the inclusion of a $\pm$ 2% error in the partial theoretical L-subshell ICC.

Figure 14. Ratios of Sliv's and Rose's theoretical L-subshell ICC for M1 and E2 transitions for k = 0.1 plotted against the atomic number, Z.

Figure 15. Ratios of Sliv's and Rose's theoretical L-subshell ICC for M1 and E2 transitions for Z = 70 plotted against the transition energy k.

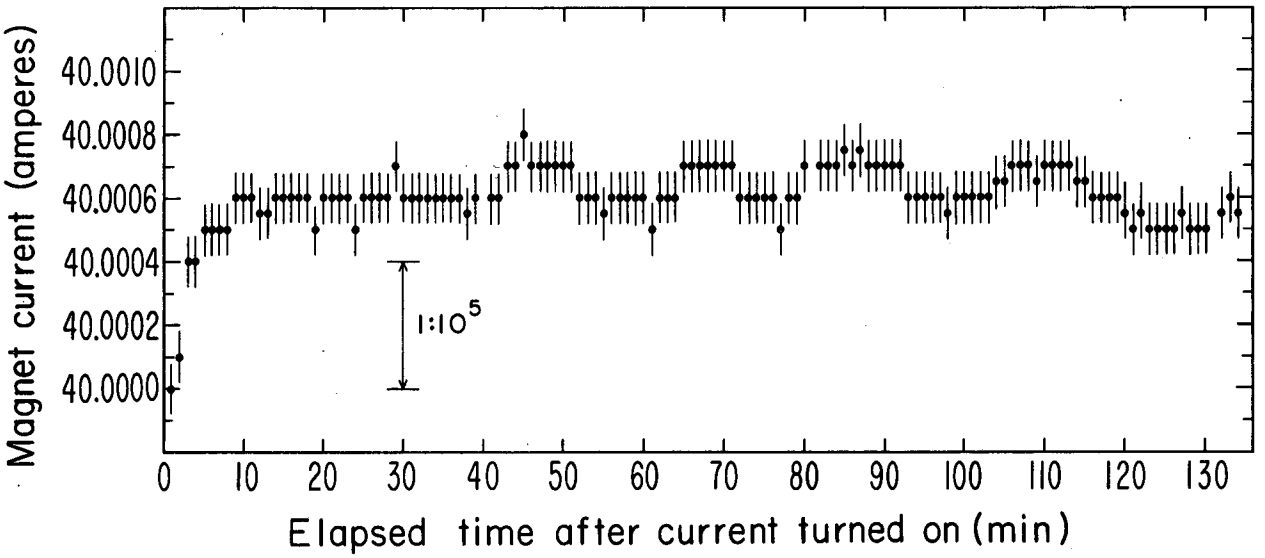

MUB-2841

Fig. 1.

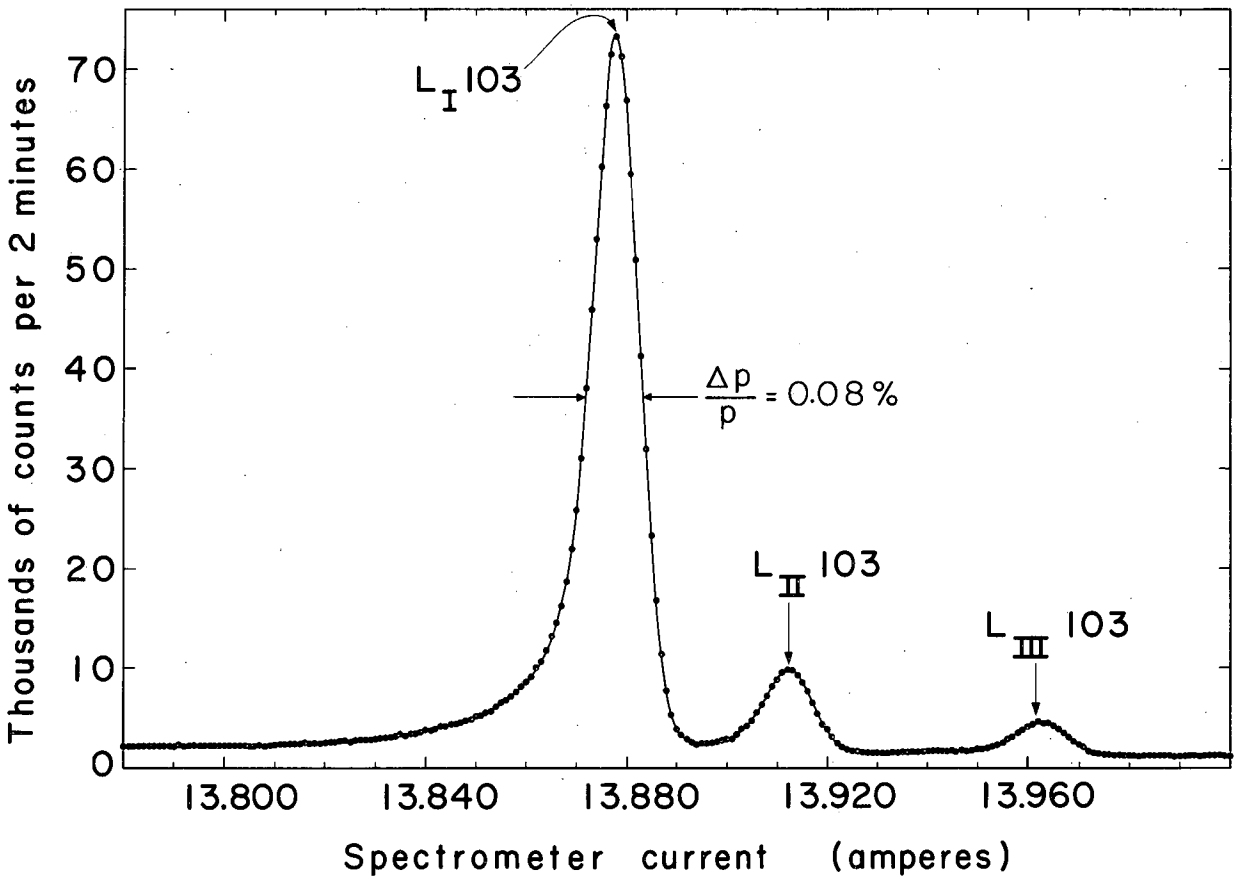
Thousands of counts per 2 minutes
0
10
20
30
40
50
60
70
L_I 103
$\frac{\Delta p}{p}$ = 0.08 %
L_{II} 103
L_{III} 103
13.800
13.840
13.880
13.920
13.960
Spectrometer current (amperes)
MUB-2184

Fig. 2.

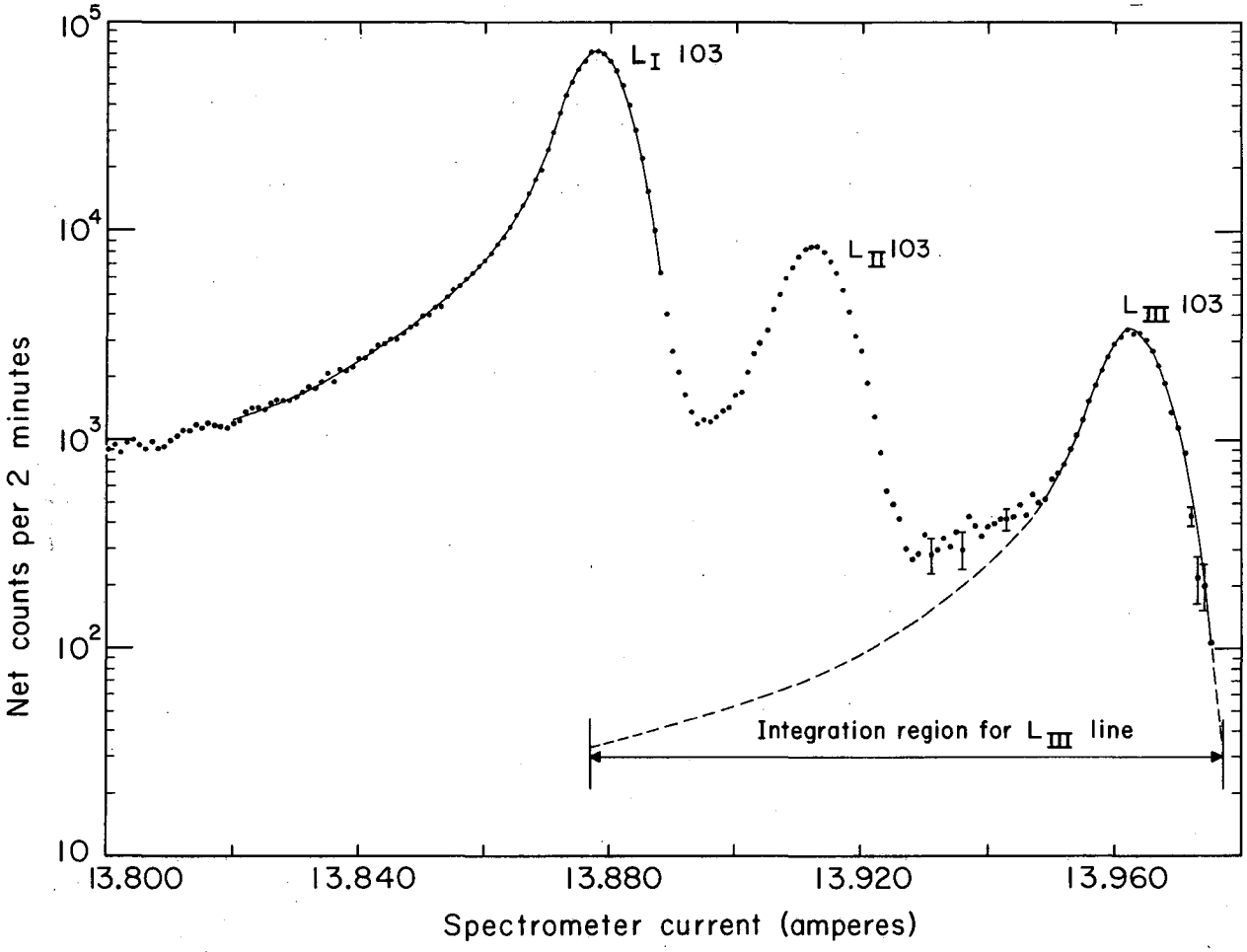
10^5
10^4
10^3
10^2
10
Net counts per 2 minutes
L_I 103
L_{II} 103
L_{III} 103
Integration region for L_{III} line
13.800
13.840
13.880
13.920
13.960
Spectrometer current (amperes)
MUB-2842

Fig. 3.

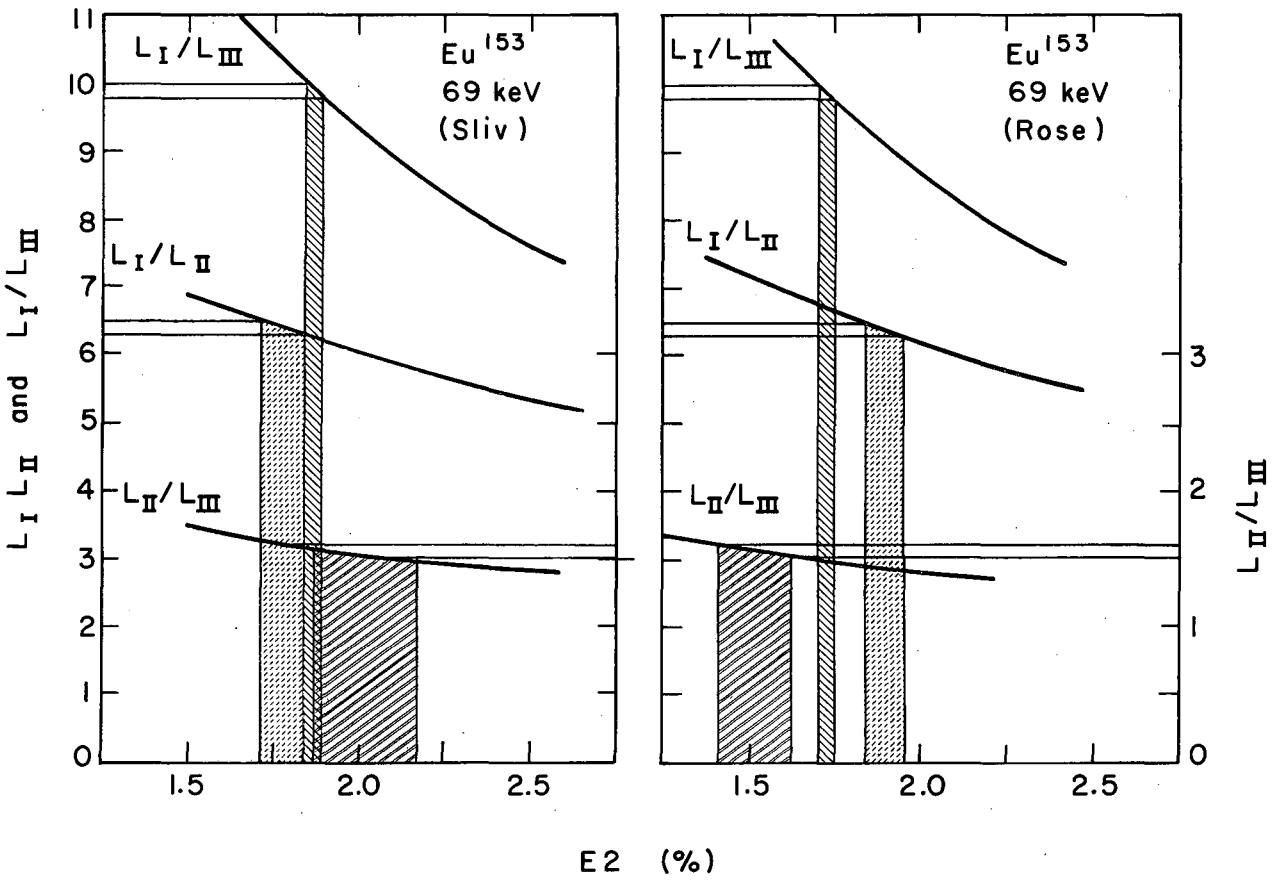
L_I/L_{III}
Eu^{153}
69 keV
(Sliv)
L_I/L_{II}
L_{II}/L_{III}
L_I/L_{III}
Eu^{153}
69 keV
(Rose)
L_I/L_{II}
L_{II}/L_{III}
L_I L_{II} and L_I/L_{III}
L_{II}/L_{III}
E2 (%)
MUB-2484

Fig. 4.

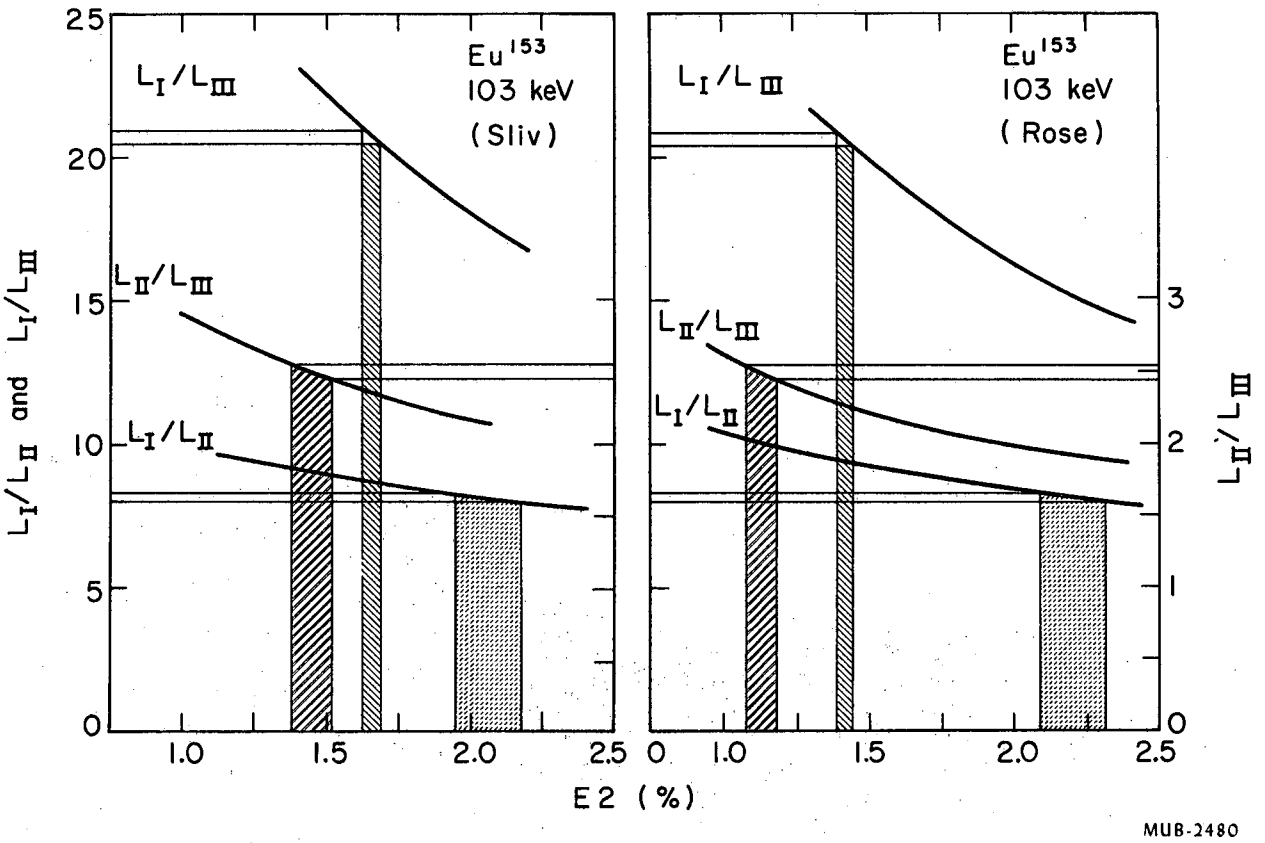
L_I/L_{III}
Eu^{153}
103 keV
(Sliv)
L_{II}/L_{III}
L_I/L_{II}
L_I/L_{II} and L_I/L_{III}
L_I/L_{III}
Eu^{153}
103 keV
(Rose)
L_{II}/L_{III}
L_I/L_{II}
L_{II}/L_{III}
E2 (%)
MUB-2480

Fig. 5.

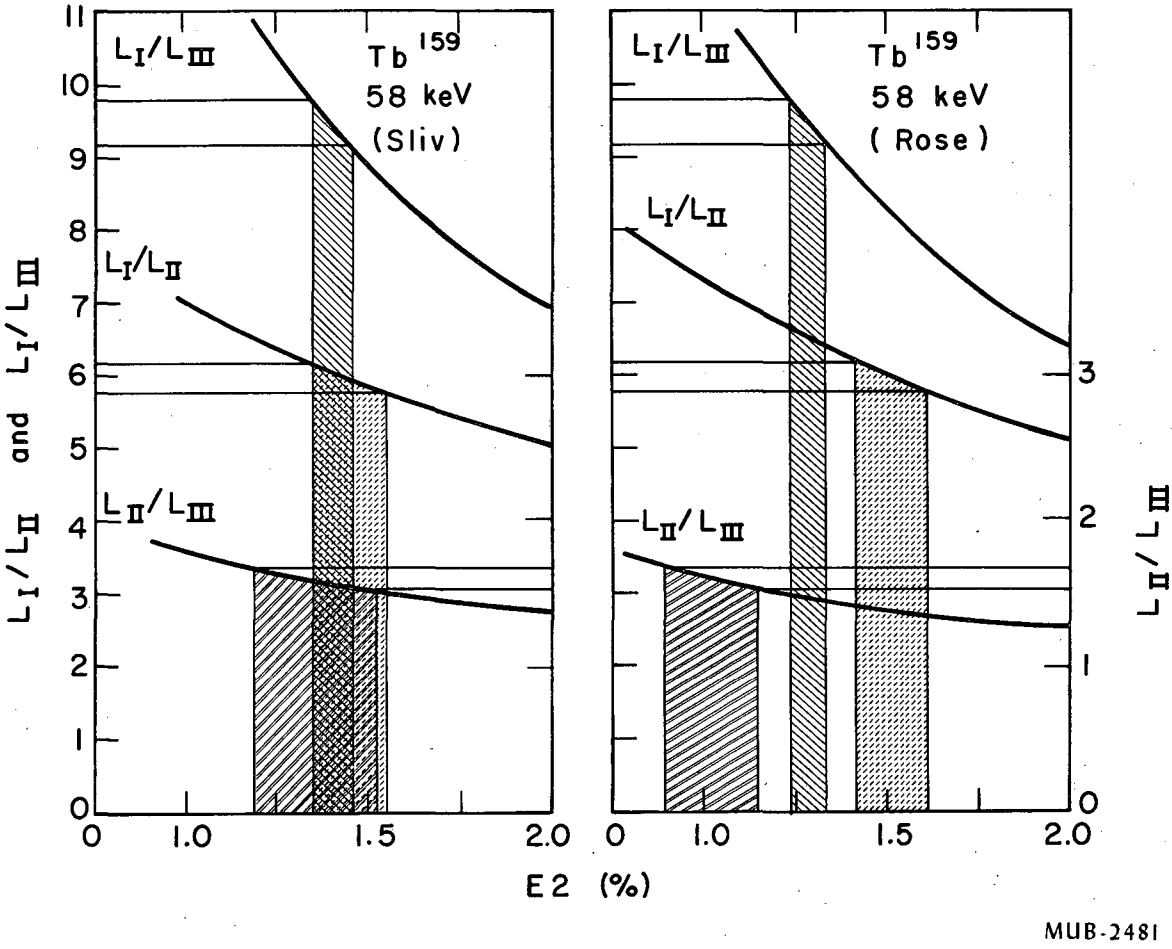
L_I/L_{III}
Tb^{159}
58 keV
(Sliv)
L_I/L_{II}
L_{II}/L_{III}
L_I/L_{II} and L_I/L_{III}
L_{II}/L_{III}
E2 (%)
MUB-2481

Fig. 6.

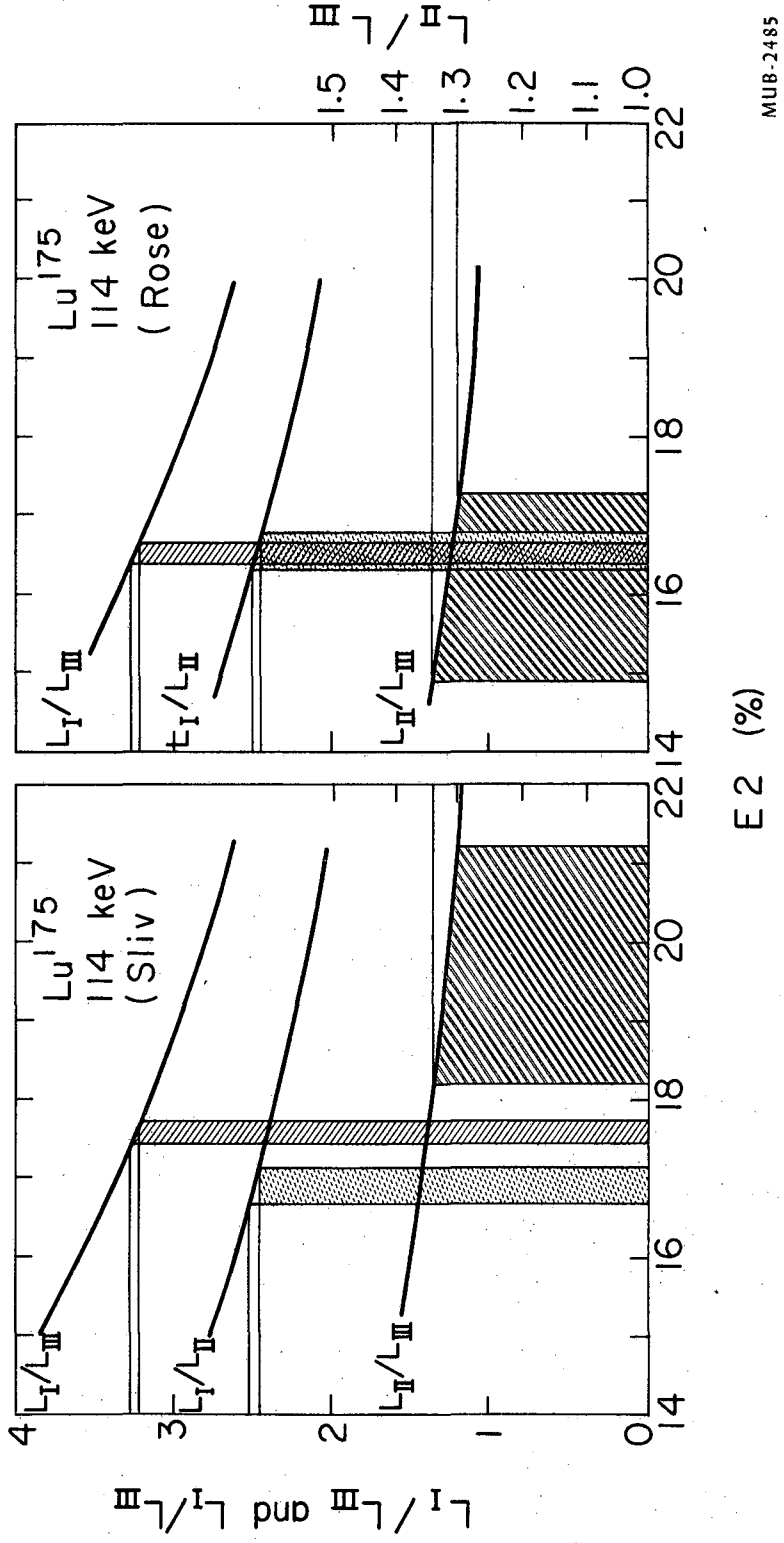
Lu175
114 keV
(Sliv)
Lu175
114 keV
(Rose)
LI/LIII
LI/LII
LII/LIII
LI / LIII and LI/LIII
LIII / LII
E2 (%)
MUB-2485

Fig. 7.

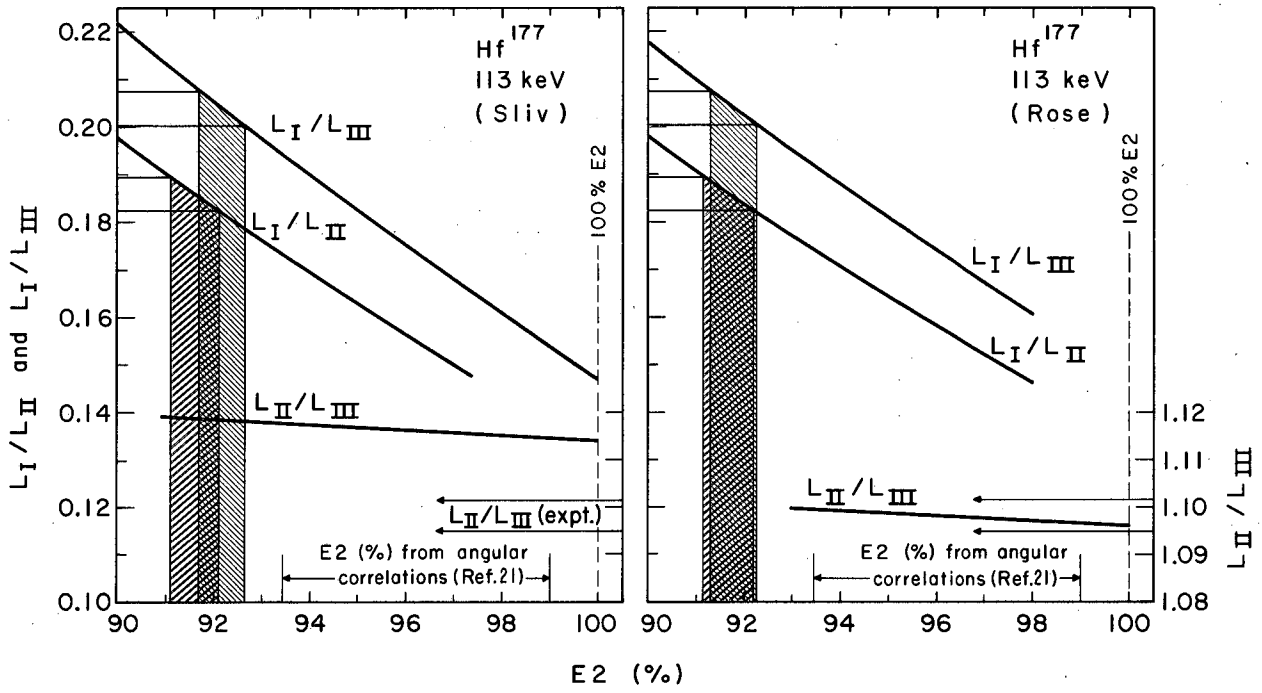

MUB-2843

Fig. 8.

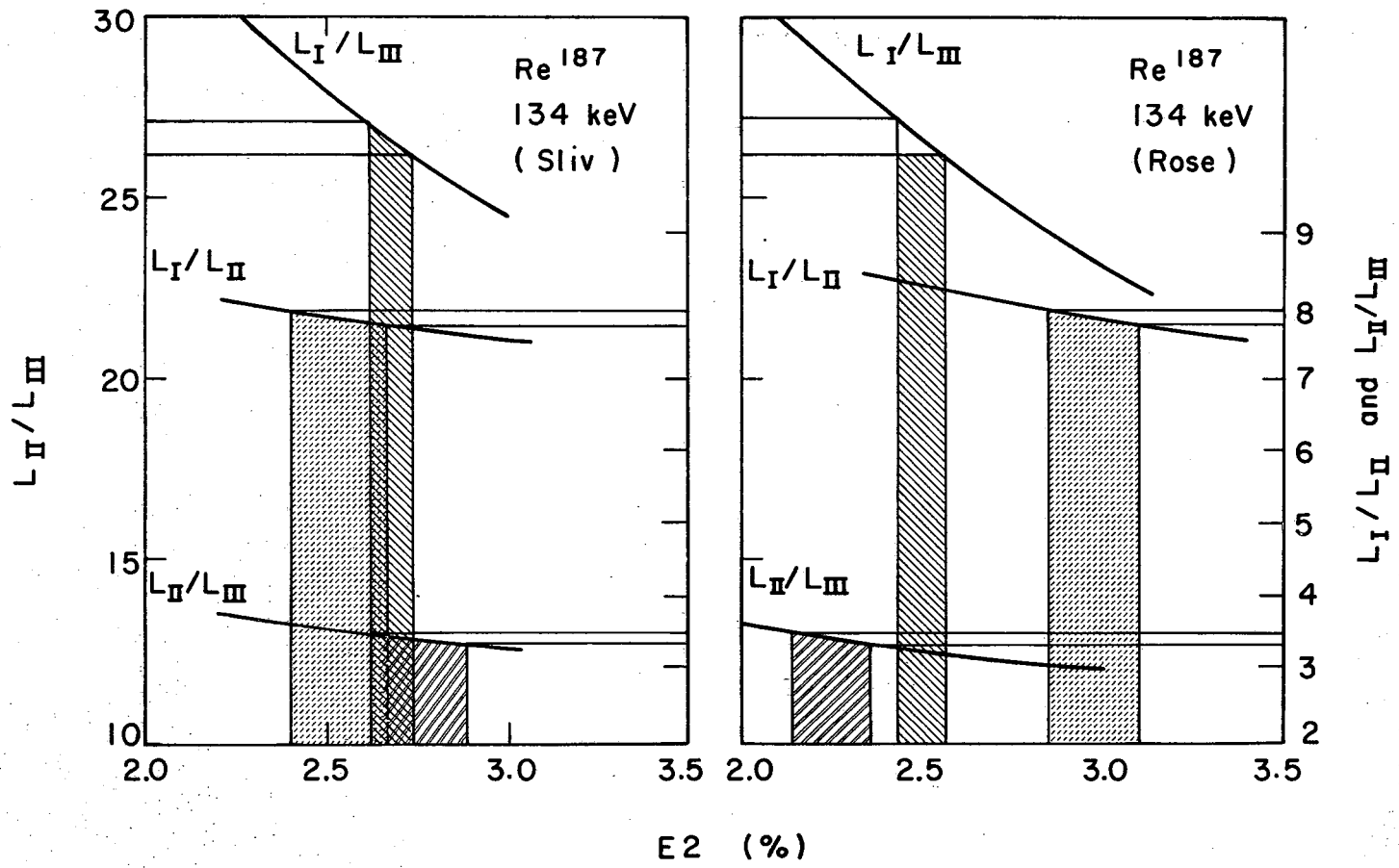
30
25
20
15
10
2.0
2.5
3.0
3.5
L_I/L_{III}
L_I/L_{II}
L_{II}/L_{III}
Re 187
134 keV
(Sliv)
Re 187
134 keV
(Rose)
9
8
7
6
5
4
3
2
L_{II}/L_{III}
L_I/L_{II} and L_I/L_{III}
E2 (%)
MUB-2482

Fig. 9.

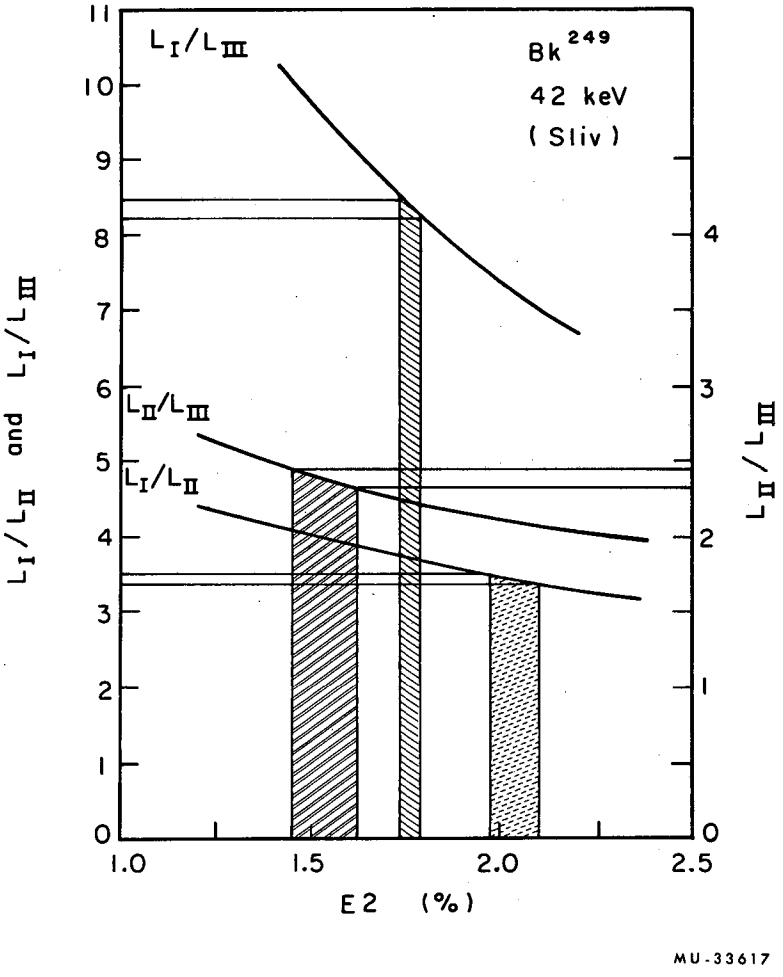
L_I/L_{III}
Bk^{249}
42 keV
(Sliv)
L_{II}/L_{III}
L_I/L_{II}
L_I/L_{II} and L_I/L_{III}
L_{II}/L_{III}
E2 (%)
MU-33617

Fig. 10.

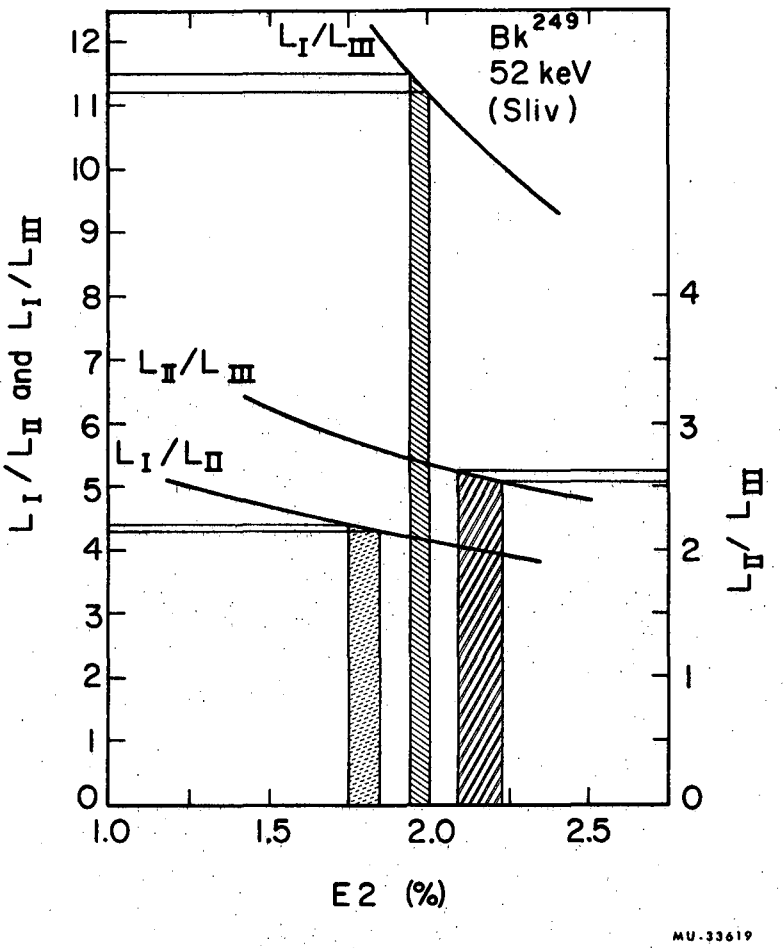
L_I/L_{III}
Bk^{249}
52 keV
(Sliv)
L_{II}/L_{III}
L_I/L_{II}
L_I/L_{II} and L_I/L_{III}
L_{II}/L_{III}
E2 (%)
MU-33619

Fig. 11.

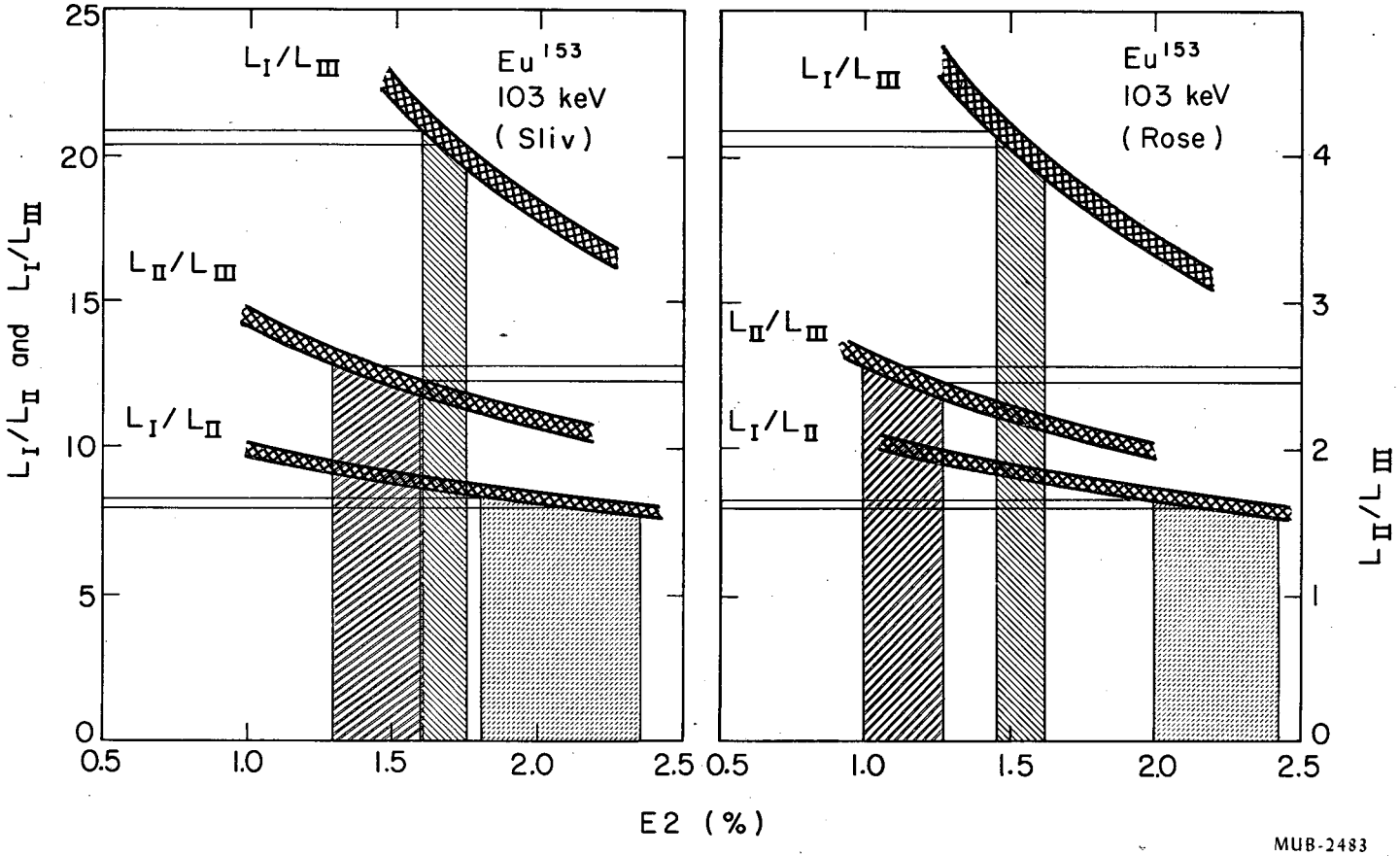
L_I/L_{III}
Eu^{153}
103 keV
(Sliv)
L_{II}/L_{III}
L_I/L_{II}
L_I/L_{II} and L_I/L_{III}
L_I/L_{III}
Eu^{153}
103 keV
(Rose)
L_{II}/L_{III}
L_I/L_{II}
L_{II}/L_{III}
E2 (%)
MUB-2483

Fig. 12.

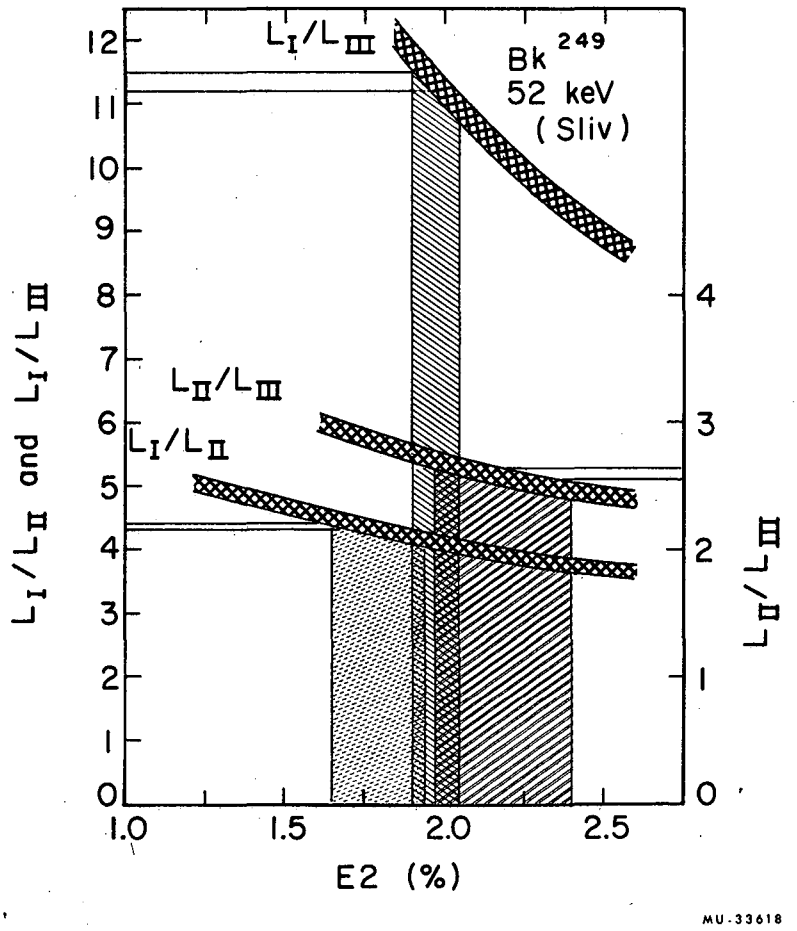
L_I/L_{III}
Bk 249
52 keV
(Sliv)
L_{II}/L_{III}
L_I/L_{II}
L_I/L_{II} and L_I/L_{III}
L_{II}/L_{III}
E2 (%)
MU-33618

Fig. 13.

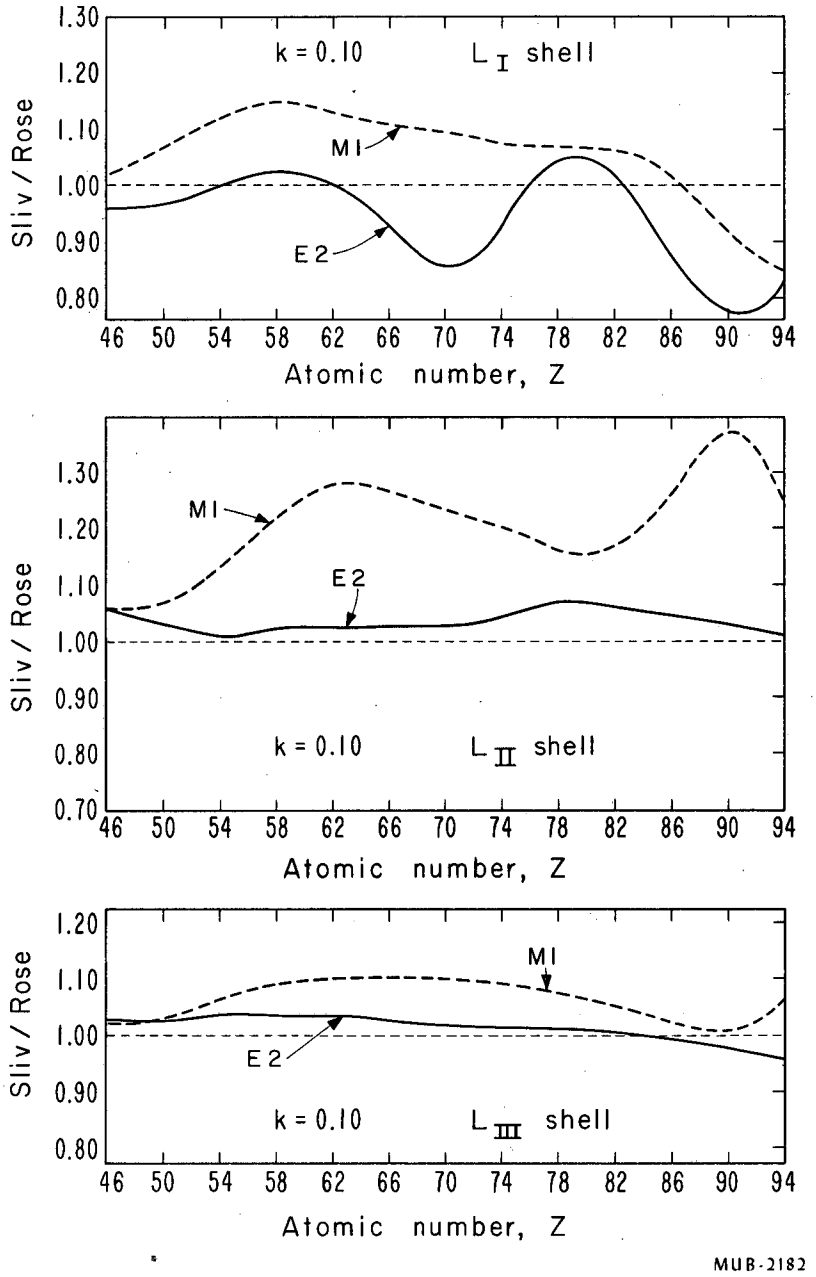
Sliv / Rose
1.30
1.20
1.10
1.00
0.90
0.80
k = 0.10
L_I shell
M1
E2
46 50 54 58 62 66 70 74 78 82 86 90 94
Atomic number, Z
Sliv / Rose
1.30
1.20
1.10
1.00
0.90
0.80
0.70
M1
E2
k = 0.10
L_{II} shell
46 50 54 58 62 66 70 74 78 82 86 90 94
Atomic number, Z
Sliv / Rose
1.20
1.10
1.00
0.90
0.80
M1
E2
k = 0.10
L_{III} shell
46 50 54 58 62 66 70 74 78 82 86 90 94
Atomic number, Z
MUB-2182

Fig. 14.

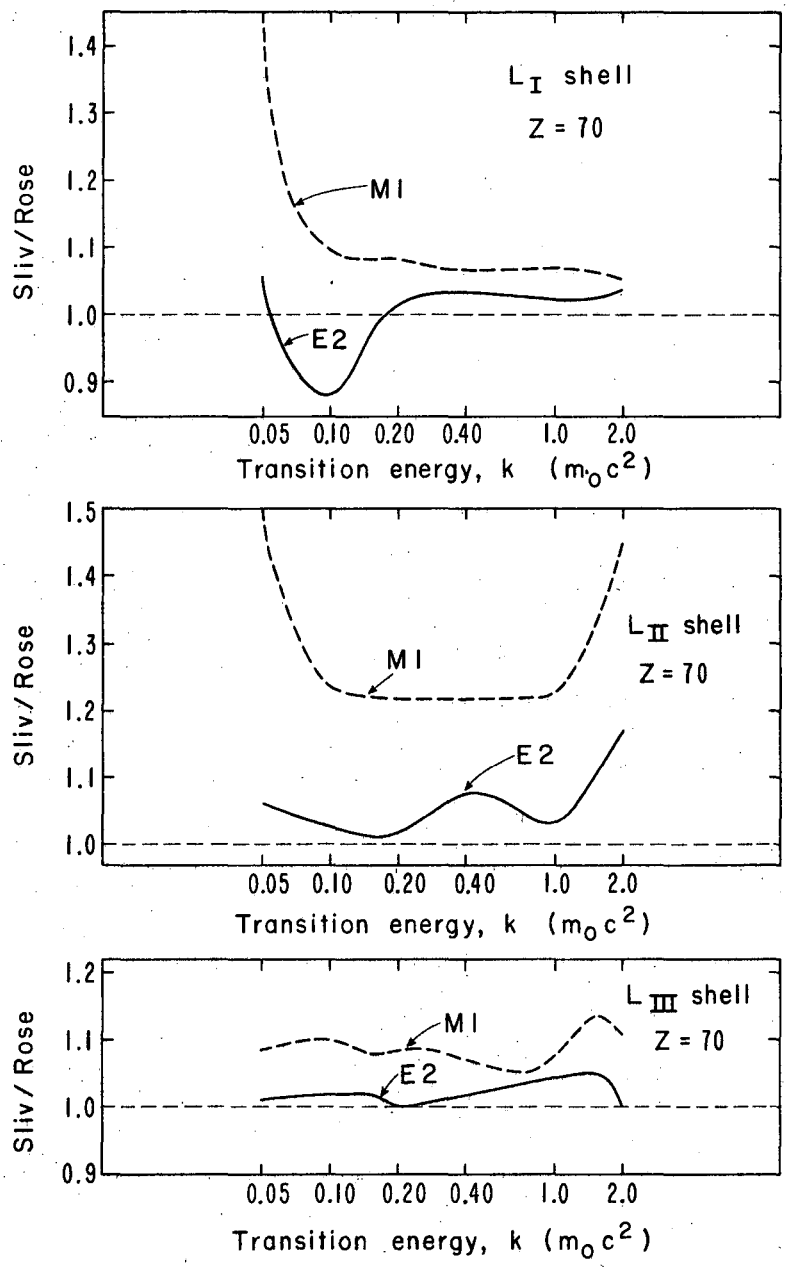
Sliv/Rose
1.4
1.3
1.2
1.1
1.0
0.9
L_I shell
Z = 70
M1
E2
0.05 0.10 0.20 0.40 1.0 2.0
Transition energy, k (m_0c^2)
Sliv/Rose
1.5
1.4
1.3
1.2
1.1
1.0
M1
L_{II} shell
Z = 70
E2
0.05 0.10 0.20 0.40 1.0 2.0
Transition energy, k (m_0c^2)
Sliv/Rose
1.2
1.1
1.0
0.9
M1
L_{III} shell
Z = 70
E2
0.05 0.10 0.20 0.40 1.0 2.0
Transition energy, k (m_0c^2)
MUB-2844

Fig. 15.